Onset of fractional-order thermal convection in porous media

Hamid Karani, Majid Rashtbehesht, Christian Huber, and Richard L. Magin

Phys. Rev. E **96**, 063105 — Published 6 December 2017

DOI: 10.1103/PhysRevE.96.063105

Onset of fractional-order thermal convection in porous media

Hamid Karani
*School of Earth & Atmospheric Sciences, Georgia Institute of Technology**

Majid Rashtbehesht and Christian Huber
Department of Earth, Environmental and Planetary Sciences, Brown University

Richard L. Magin
Department of Bioengineering, University of Illinois at Chicago
(Dated: November 20, 2017)

The macroscopic description of buoyancy-driven thermal convection in porous media is governed by advection-diffusion processes, which in the presence of thermophysical heterogeneities fail to predict the onset of thermal convection and the average rate of heat transfer. This work extends the classical model of heat transfer in porous media by including a fractional-order advective-dispersive term to account for the role of thermophysical heterogeneities in shifting the thermal instability point. The proposed fractional-order model overcomes limitations of the common closure approaches for the thermal dispersion term by replacing the diffusive assumption with a fractional-order model. Through a linear stability analysis and Galerkin procedure, we derive an analytical formula for the critical Rayleigh number as a function of the fractional model parameters. The resulting critical Rayleigh number reduces to the classical value in the absence of thermophysical heterogeneities when solid and fluid phases have similar thermal conductivities. Numerical simulations of the coupled flow equation with the fractional-order energy model near the primary bifurcation point confirm our analytical results. Moreover, data from pore-scale simulations are used to examine the potential of the proposed fractional-order model in predicting the amount of heat transfer across the porous enclosure. The linear stability and numerical results show that, unlike the classical thermal advection-dispersion models, the fractional-order model captures the advance and delay in the onset of convection in porous media and provides correct scalings for the average heat transfer in a thermophysically heterogeneous medium.

I. INTRODUCTION

The dynamics of transport processes in porous media is usually characterized by early/late arrivals (heavy tails) in the breakthrough curves of the advective species [1] and a nonlinear mean-squared displacement (MSD) for the growth of the spreading entities in diffusive systems [2–4]. These features of transport behaviors have been observed in natural and engineered heterogeneous systems, including the transport of passive tracers in subsurface media [5, 6], diffusion in gels [7, 8], MRI diffusion processes in biological tissues [9, 10], infiltration of moisture in porous media [11–13], and Turing pattern formation in reaction-diffusion systems [14–16]. The heterogeneous and disordered microstructure in these media creates complex transport pathways, such as low mobility zones, dead ends and preferential paths. The upscaling of these localized retardation and enhancement transport zones leads to anomalous transport behaviors that deviate from the classical advection-dispersion regimes.

Heat transfer processes in porous media, such as forced thermal convection and natural thermally-driven flows, can also exhibit anomalous behaviors. In the former, in analogy with solute transport in porous media, Continuous Time Random Walk (CTRW) models [17, 18] and fractional-order energy models [19, 20] have been developed and tested for modeling the experimentally and numerically observed heavy-tailed thermal breakthrough curves due to structural heterogeneities. In the buoyancy-driven thermal convection, also known as Horton-Rogers-Lapwood convection [21, 22] (in short HRL), the anomalous behavior, however, can occur even in a ordered homogeneous and isotropic porous matrix and it manifests itself in shifts for (1) the critical Rayleigh number at the onset of thermal instability, and (2) the average heat transfer represented by the Nusselt-Rayleigh number correlation [23, 24]. In the absence of an inclusive model that can explain these two deviations from the standard solution for HRL convection, Karani and Huber [25] argued for the need to revisit the closure of the thermal dispersion term, which arises from upscaling of the velocity and temperature fluctuation fields [26, 27]. Thermal dispersion is historically modeled as a diffusive formulation (originally suggested by Taylor [28] and later extended by Aris [29], Saffman [30, 31], Poreh [32]).

In analogy with the fractional-order advection-dispersion models for anomalous solute transport regimes in porous media [5, 33, 34], one can use a fractional-order thermal advection-dispersion model for describing HRL convection. The main difference is that, in solute transport in porous media, the anomalous dispersion due to the velocity and concentration fluctuations originates from the structural disorder and heterogeneties, while in HRL convection, the thermophysical heterogeneity, i.e.

* hamid.karani@gatech.edu

contrast in thermal conductivities of the solid and fluid phases, can also be responsible for the resulting anomalous thermal behaviors [25]. Thermophysical heterogeneities are ubiquitous in almost every multi-component and multi-phase systems, and are responsible for partitioning of energy among the different constituents.

The present study investigates how a fractional-order energy model influences the onset of instability in HRL convection. We perform a linear stability analysis and derive an analytical expression for the critical Rayleigh number as a function of the fractional-order parameters that govern the conservation equation. We also solve numerically the original nonlinear coupled equations of motion and fractional heat transfer and verify the robustness of the linear stability results. The linear stability and numerical results show that the fractional-order energy formulation can be successfully and consistently used for modeling the scatter of the onset of instability in HRL convection observed experimentally in Cheng [23], Kladias and Prasad [24] and reported from direct numerical simulations by Karani and Huber [25].

II. MATHEMATICAL FORMULATION

We consider a two-dimensional fluid-saturated porous square domain with dimensions $0 < x < H$ and $0 < y < H$, where H is the height/length of the porous enclosure. While the linear stability analysis can be naturally exended to three-dimensions, in order to benefit from the results of an equivalent pore-scale study [25], we limit our analysis to two dimensions. Assuming a Darcian regime, continuity and momentum equations of a Boussinesq fluid in an isotropic porous medium are described, at the continuum scale, by [35]:

$$\frac{\partial u}{\partial x} + \frac{\partial v}{\partial y} = 0, \tag{1}$$

$$u = -\frac{K}{\mu}\frac{\partial P}{\partial x}, \tag{2}$$

$$v = -\frac{K}{\mu}\frac{\partial P}{\partial y} + \frac{\rho g \beta K}{\mu}(T - T_{ref}), \tag{3}$$

where u and v are Darcy-scale macroscopic velocities in the x- and y-directions, respectively. T and T_{ref} are local average-scale temperature and the reference temperature for the fluid density, respectively. Also, ρ, β, K and g are the fluid density, thermal expansion coefficient, permeability of the porous medium and and acceleration of gravity; P is pressure and μ is the dynamic viscosity of the fluid.

Under the assumption of local thermal equilibrium between the solid and fluid phases, the average-scale energy equation for HRL convection takes the following form:

$$(\rho c)_m \frac{\partial T}{\partial t} + (\rho c)_f \mathbf{V}\cdot\nabla T + (\rho c)_f \nabla\cdot(< \mathbf{V}'T' >^f) = k_m \nabla^2 T, \tag{4}$$

where $\mathbf{V}$ is the velocity vector (u, v), c is the specific heat, k_m is the stagnant thermal conductivity of the solid/fluid mixture. The subscripts m and f refer to the properties of the solid/fluid mixture and the fluid, respectively. The $\nabla\cdot((\rho c)_f < \mathbf{V}'T' >^f)$ term describes the thermal dispersion term, with the primes indicating the fluctuating fields with respect to the fluid-phase averaged value of the local temperature and velocity fields (for the detailed derivations, the reader is referred to Refs. [26, 27]). Closure models for thermal dispersion often assume a pseudo-diffusive behavior [28, 30–32], i.e. $\nabla\cdot[(\rho c)_f < \mathbf{V}'T' >^f] = \nabla\cdot(-k_{dis}\nabla T)$. Here, k_{dis} is the dispersive conductivity of the porous media, which is generally a nonlinear function of the pore-scale Péclet or Reynolds number based on the local average velocity of the fluid [28, 30–32].

In the present study, in analogy with fractional-order advective-dispersive solute transport equation, we replace Eq. 4 with the following energy equation with a fractional-order advective term:

$$(\rho c)_m \frac{\partial T}{\partial t} + (\rho c)_f \hat{C}_{dis} \mathbf{V}\cdot\nabla^\alpha T = k_m \nabla^2 T. \tag{5}$$

$\hat{C}_{dis}$ ($[L^{\alpha-1}]$) is the dispersive coefficient and α is the fractional-derivative index based on the Riemann-Liouville definition [36]:

$$\frac{d^\alpha \Phi}{dz^\alpha} = \frac{d^n}{dz^n}\int_0^z \frac{(z-\xi)^{n-\alpha-1}}{\Gamma(n-\alpha)}\Phi d\xi, \tag{6}$$

where $n - 1 < \alpha < n$ and n is the integer and $\Gamma(.)$ is the Gamma function.

The pore-scale modeling results in Karani and Huber [25] suggest that the thermal dispersion originates from thermophysical heterogeneities in a porous medium (i.e. differences in solid and fluid thermal conductivities). It exhibits some intermediate behaviors, which cannot be fully taken into account as a pure diffusive form. Karani and Huber [25] further suggested that the diffusive nature of the often assumed thermal dispersion term is responsible for the observed inconsistencies in the thermal predictions for the onset of convection and Nusselt-Rayleigh scalings. The rationale behind using a fractional-order advective-dispersive equation is to relax this *a priori* diffusive assumption for the thermal dispersion term. Accordingly, we assume that the contribution of $\nabla\cdot((\rho c)_f < \mathbf{V}'T' >^f)$ is to enhance or impede the overall average-scale advective thermal flux and is modeled through a fractional-order index α, which can conveniently range from advective to diffusive regimes in a flexible manner. In light of the pore-scale results of Karani and Huber [25], we argue that the fractional-order

parameters $\hat{C}_{dis}$ and α are functions of the degree of thermophysical heterogeneity, i.e. difference in solid-to-fluid thermal conductivity ratio k_s/k_f, where k_s and k_f are thermal conductivities of the solid and fluid phases, respectively. Furthermore, Eq. 5 implies that the conductive part is consistently captured through the definition of stagnant thermal conductivity of the medium k_m. This allows Eq. 5 to successfully recover the exact conduction solution for Rayleigh numbers below the critical value.

We define the following dimensionless variables in order to recast the governing equations 1-5 in a dimensionless form:

$$\begin{aligned} t^* = t\frac{\alpha_m}{H^2\sigma}, \quad (u,v)^* = (u,v)\frac{H}{\alpha_m} \\ (x,y)^* = (x,y)\frac{1}{H}, \\ \sigma = \frac{(\rho c)_m}{(\rho c)_f}, \quad \theta = \frac{T-T_{ref}}{T_h - T_c}, \end{aligned} \tag{7}$$

where $\alpha_m = k_m/(\rho c)_f$ is the thermal diffusivity of the porous medium based on the stagnant thermal conductivity k_m. $(\rho c)_f$ is the volumetric heat capacity (density times specific heat) of the fluid phase. Also, H is the characteristic height of the porous enclosure.

We use the stream function ψ and normalize lengths, velocity, time and temperature based on the dimensionless variables in Eq. 7 to retrieve the following dimensionless momentum and energy equations (dropping asterisk for simplicity):

$$\frac{\partial^2\psi}{\partial x^2} + \frac{\partial^2\psi}{\partial y^2} = Ra\frac{\partial\theta}{\partial x}, \tag{8}$$

$$\frac{\partial\theta}{\partial t} + C_{dis}(u\frac{\partial^\alpha\theta}{\partial x^\alpha} + v\frac{\partial^\alpha\theta}{\partial y^\alpha}) = \frac{\partial^2\theta}{\partial x^2} + \frac{\partial^2\theta}{\partial y^2}, \tag{9}$$

where

$$\begin{aligned} C_{dis} = \hat{C}_{dis}\frac{H^2}{H^{1+\alpha}} \\ \mathbf{V} = (u,v) = (-\frac{\partial\psi}{\partial y}, \frac{\partial\psi}{\partial x}), \end{aligned} \tag{10}$$

and the Rayleigh number (Ra) is defined as:

$$Ra = \frac{\rho g\beta\Delta T K H}{\mu\alpha_m}. \tag{11}$$

where $\Delta T = T_h - T_c$ is the temperature difference across the porous domain.

Without losing generality, we perform the linear stability analysis of the fractional-order HRL convection for a square box. Figure 1 shows the schematic of the problem. The hydrodynamic and thermal boundary conditions are as follows:

$$(u,v) = 0, \quad \theta = 1, \quad \text{for} \quad y = 0, \quad \text{for all} \quad x, \tag{12}$$

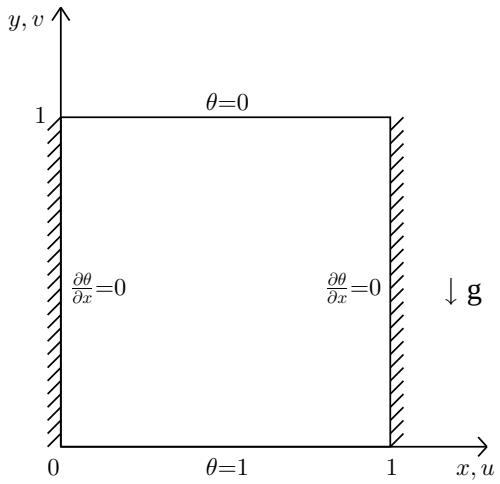

FIG. 1: Schematic showing a saturated porous square enclosure and the choice of thermal boundary conditions. No-slip velocity i.e. $(u, v{=}0)$ is applied at all the walls.

$$(u,v) = 0, \quad \theta = 0, \quad \text{for} \quad y = 1, \quad \text{for all} \quad x, \tag{13}$$

$$(u,v) = 0, \quad \frac{\partial\theta}{\partial x} = 0, \quad \text{for} \quad x = 0, 1, \quad \text{for all} \quad y. \tag{14}$$

Fractional-order derivatives are nonlocal by essence and in general, special treatments are needed when applying the boundary conditions. In the present model, the fractional-order operator is applied on the advective flux on the left-hand-side of the Eq. 5, while the diffusive term on the right-hand-side is the normal integer-order (∇^2) spatial derivative. Since we imposed a no-slip velocity on all the solid walls, the advective flux (the fractional-order term) disappears at solid boundaries. Therefore, the constant temperature and zero-flux boundary conditions are treated as in the normal diffusion problem.

In addition to the linear stability analysis, we solve the dimensionless coupled nonlinear Eqs. 8 and 9 numerically to verify the linear stability analysis. For this purpose, we use the numerical approach based on a fast Fourier transform detailed in Karani and Huber [37]. For ψ, we use a central finite difference scheme on space derivatives and treat the source term in Eq. 8 explicitly. The same procedure is used for the temperature field by treating the advective terms in Eq. 9 explicitly and the diffusion term implicitly. There are several ways to discretize the fractional-order advective terms in Eq. 9. We employ the Grünwald-Letnikov discretized representation of the Riemann-Liouville operators in Eq. 9 [36]:

$$\frac{d^\alpha\Phi}{dx^\alpha} \approx \Delta x^{-\alpha}\sum_{l=0}^{N}\omega_l\Phi(x - l\Delta x), \tag{15}$$

where Δx is the spatial grid size, and the coefficients ω_l are calculated through the following formula [36]:

$$\omega_l = \frac{(-1)^l \Gamma(\alpha+1)}{\Gamma(\alpha-l+1)l!}, \quad l = 0, 1, 2, ..., N. \tag{16}$$

Based on the resulting steady-state temperature and velocity fields of the dimensionless equations 8 and 9 at each Rayleigh number, we calculate the average amount of heat transfer across the porous enclosure through the dimensionless Nusselt number:

$$Nu = \int_0^1 -\frac{\partial T}{\partial y}\bigg|_{wall} \quad dx, \tag{17}$$

where the partial derivatives are evaluated at the horizontal bottom boundary of the porous domain.

III. LINEAR STABILITY ANALYSIS

For Rayleigh numbers below a critical value, only the conduction solution with a linear temperature profile can exist as a stable state in HRL problem (Fig. 2-(a)). As the Rayleigh number goes beyond the critical value, convection initiates (Fig. 2-(b) illustrates the 1^{st} stable convection mode). Similar to Rayleigh-Bénard convection, HRL convection allows multiplicity of stable states; meaning that several stable convection states with different wave-modes can co-exist [37–42]. In the present stability study of HRL convection, we are interested in identifying the primary bifurcation point for the onset of convection from the conduction state.

Linearization

In the absence of convection, Eqs. 8 and 9 admit the following basic conduction solution:

$$\psi = 0, \quad \theta = 1 - y. \tag{18}$$

In order to investigate the onset of convection, we consider the stability of the basic conduction solution with respect to perturbations of the form:

$$\psi = \Psi, \quad \theta = 1 - y + \Theta. \tag{19}$$

Inserting these perturbed velocity and temperature fields into Eqs. 8-9 and linearizing the nonlinear advective terms gives the following set of linearized equations:

$$\frac{\partial^2 \Psi}{\partial x^2} + \frac{\partial^2 \Psi}{\partial y^2} = Ra \frac{\partial \Theta}{\partial x}, \tag{20}$$

$$\frac{\partial \Theta}{\partial t} - C_{dis}\frac{\partial \Psi}{\partial y}\frac{\partial^\alpha (1-y)}{\partial x^\alpha} + C_{dis}\frac{\partial \Psi}{\partial x}\frac{\partial^\alpha (1-y)}{\partial y^\alpha} = \frac{\partial^2 \Theta}{\partial x^2} + \frac{\partial^2 \Theta}{\partial y^2}. \tag{21}$$

Compared with the classical integer-order counterpart, introducing a Riemann-Liouville fractional-order advective term results in an additional linearized advective term in Eq. 21. This is due to the fact that the fractional-order derivative of a constant is not zero in the Riemann-Liouville definition [36]; in other words, $\alpha-$ order derivative of a $(1-y)$ with respect to x has nonzero values. More specifically, the analytical relations for the fractional-order derivative terms in Eq. 21 are [36]:

$$\frac{\partial^\alpha (1-y)}{\partial x^\alpha} = (1-y)\frac{x^{-\alpha}}{\Gamma(1-\alpha)}, \tag{22}$$

$$\frac{\partial^\alpha (1-y)}{\partial y^\alpha} = \frac{y^{-\alpha}}{\Gamma(1-\alpha)} - \frac{y^{-\alpha+1}}{\Gamma(2-\alpha)}. \tag{23}$$

Galerkin method

We find the onset of the convective instability by solving for the eigenvalue of the coupled partial differential equations 20 and 21. Because of the variable coefficients for the advective terms in Eq. 21, we select the Galerkin procedure to solve this eigenvalue problem [43, 44]. We use the following trial functions for the velocity and temperature fields, which automatically satisfy the thermal and hydrodynamic boundary conditions in Eqs. 12-14:

$$\begin{aligned} \Psi &= \sum_{m=1}^{M}\sum_{n=1}^{N} a_{mn} \sin(m\pi x)\sin(n\pi y), \\ \Theta &= \sum_{m=1}^{M}\sum_{n=1}^{N} b_{mn} \cos(m\pi x)\sin(n\pi y). \end{aligned} \tag{24}$$

We substitute these trial functions in the linearized perturbation Eqs. 20 and 21 to find the residuals. We then orthogonalize the residuals (in the spatial domain) with respect to each trial functions, which provides the generalized algebraic eigenvalue problem, where the lowest eigenvalue is the critical Rayleigh number.

We initially limit the analysis to the first order approximation of the Galerkin method, since it conveniently provides a closed form relation for the critical Rayleigh number. The details for the second order approximation are provided in the Appendix. In the results section, we will show that the first term approximation provides accurate values.

Considering only the lowest order values for M and N in Eq. 24 ($M = N = 1$), we retrieve:

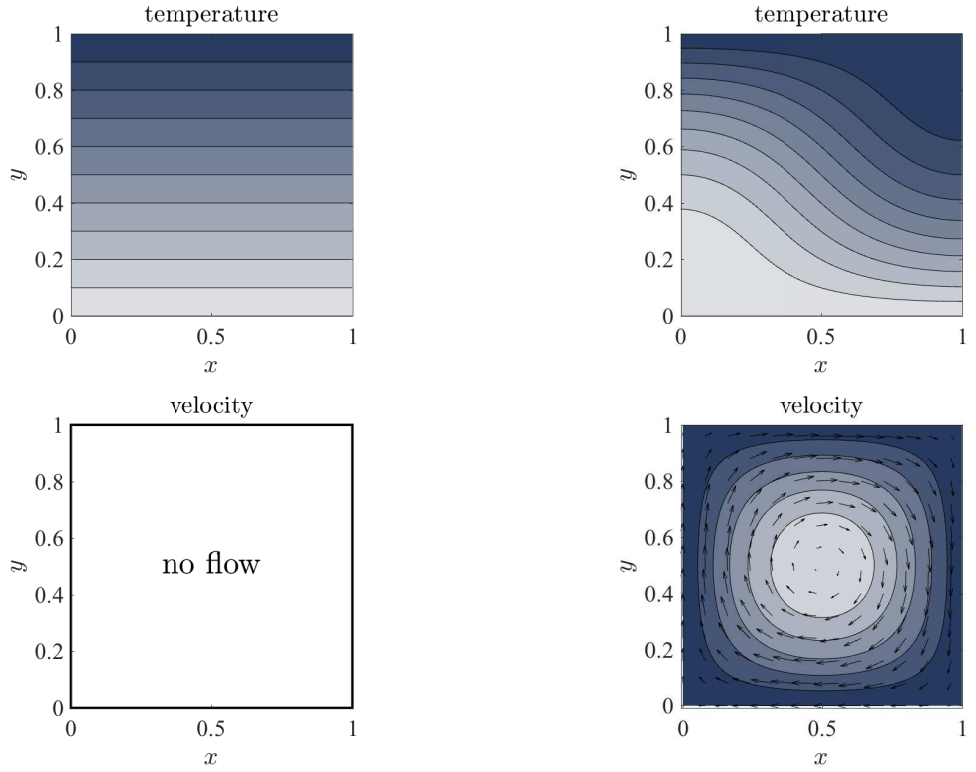

(a) conduction state: $Ra < Ra_{cr}$

(b) convection state: $Ra > Ra_{cr}$

FIG. 2: Schematic showing the conduction (panel (a)) and convection stable states (panel (b)) for Rayleigh numbers below and above the critical value, respectively.

$$\begin{aligned} \Psi &= a_{11}\sin(\pi x)\sin(\pi y), \\ \Theta &= b_{11}\cos(\pi x)\sin(\pi y). \end{aligned} \tag{25}$$

Inserting these relations into the linearized perturbed equations and using their orthogonality property (details can be found for example in [44]), we arrive at the following generalized eigenvalue problem:

$$\begin{pmatrix} 2\pi^2 & -Ra\pi \\ C_2\pi & -2C_1\pi^2 \end{pmatrix} \begin{pmatrix} a_{11} \\ b_{11} \end{pmatrix} = \begin{pmatrix} 0 \\ 0 \end{pmatrix}, \tag{26}$$

where

$$C_1 = \int_0^1 \int_0^1 (\sin(\pi y)\cos(\pi x))^2 dxdy = 1/4, \tag{27}$$

$$\begin{aligned} C_2 = C_{dis}\Bigg[&\frac{1}{\Gamma(1-\alpha)} \int_0^1 \int_0^1 \frac{1-y}{x^\alpha} (\sin(\pi x)\cos(\pi y))(\sin(\pi y)\cos(\pi x)) dxdy \\ &- \frac{1}{\Gamma(1-\alpha)} \int_0^1 \int_0^1 \frac{1}{y^\alpha} (\sin(\pi y)\cos(\pi x))^2 dxdy \\ &+ \frac{1}{\Gamma(2-\alpha)} \int_0^1 \int_0^1 \frac{1}{y^{\alpha-1}} (\sin(\pi y)\cos(\pi x))^2 dxdy \Bigg], \end{aligned} \tag{28}$$

where C_2 accounts for the influence of the nonlocal advective terms. For each value of the fractional-order

derivative α, C_2 can be calculated in a straight-forward way.

The critical Rayleigh number can be determined by setting the determinant of the matrix in Eq. 26 to zero, which yields:

$$Ra_{cr} = \frac{C_1 4\pi^2}{C_2}. \tag{29}$$

The closed form relation for Ra_{cr} in Eq. 29 allows us to measure the effect of the fractional order of the advective operator on the onset of thermal convection and compare it with $4\pi^2$, which is the Ra_{cr} in the classical HRL convection in a square box [21, 22, 42, 45].

IV. RESULTS

In Fig. 3, we compare the linear stability results of HRL convection based on single- and two-term approximations in the Galerkin procedure (Eqs. A2 and A3). Having a maximum deviation of less than 1% confirms that the formula for the critical Rayleigh number in Eq. 29 based on the single-term Galerkin approximation provides accurate results. In all the cases studied here for HRL convection in a square box, the critical convection mode was always observed to be the first mode, i.e. the one shown schematically in Fig. 2-(b). Therefore, we focus on the single-term Galerkin solution 29 as the linear stability result of the fractional-order HRL problem. We notice in Fig. 3 that the fractional-order parameters α and C_{dis} can significantly shift the bifurcation point away from the $4\pi^2$ value of the classical HRL convection in a square box, i.e for the case of $C_{dis} = \alpha = 1$. This is more clearly illustrated by Fig. 4 where we show the map of Ra_{cr} for a range of fractional-order parameters. There is a general trend of increasing Ra_{cr} as we move to lower values of α for a given C_{dis}. A similar trend occurs if α is fixed, and increasing values of C_{dis} result in shifting the critical Rayleigh number to lower values.

As mentioned previously, experimental studies and pore-scale numerical simulations have reported shifts in the onset of convection (Ra_{cr}) and the heat transfer predicted at a given Ra number. The pore-scale results in [25] suggest that, for HRL convection in a homogeneous and isotropic porous medium, α and C_{dis} are related to the thermal conductivity difference between the solid and fluid phases. Based on Fig. 4, one can get a similar Ra_{cr} at the onset of convection for different combinations of fractional model parameters α and C_{dis}. However, we can provide further insight into the valid ranges of these parameters by solving numerically the coupled nonlinear equations of motion and energy, i.e. Eqs. 8 and 9 (following the procedure outlined in Section II), and comparing the resulting Nusselt number at each Ra with those from the equivalent pore-scale observations [25]. Figure 5 shows the comparison of the critical Rayleigh numbers obtained with linear stability with those retrieved numerically. The maximum relative deviation of less than 3% between the critical Rayleigh numbers from the linear stability analysis and those from the numerical solution confirms once more the accuracy of the first-term Galerkin approximation.

We extend our numerical analysis to Rayleigh numbers greater than Ra_{cr} and observe how the fractional model parameters α and C_{dis} influence the thermal behavior represented by the Nusselt-Rayleigh curve. In Fig. 6-(a), we compare the predictions from the fractional model with those from the pore-scale analysis of [25] for three different values of k_s/k_f. While the pore-scale results for $k_s/k_f = 1$ recover the classical predictions of HRL convection with $\alpha = C_{dis} = 1$, the condition $k_s/k_f > 1$ shifts the onset of convection to higher Rayleigh numbers than $4\pi^2$ and lower Nusselt numbers compared with the classical predictions. In contrast, when $k_s/k_f < 1$ results in earlier initiation of convection, i.e. Ra_{cr} smaller than $4\pi^2$ and higher Nusselt numbers compared to the classical predictions. Figure 6-(a) shows these two features for two sample sets of α and C_{dis}, each qualitatively agreeing with the corresponding pore-scale calculations. We observed that among different combinations of fractional model parameters, $\alpha < 1$ and $C_{dis} > 1$ leads to thermal behaviors which satisfy those observed for $k_s/k_f > 1$. On the other hand, when $\alpha > 1$ and $C_{dis} < 1$, the thermal behavior for the onset of convection and Nusselt-Rayleigh curve agrees with those cases where $k_s/k_f < 1$. We can apply these constraints to identify the suitable ranges of fractional model parameters α and C_{dis} for HRL convection in a homogeneous and isotropic porous medium, which is illustrated in Fig. 6-(b).

Based on the present linear stability and the numerical results, we can summarize the variations of α and C_{dis} with the thermal conductivity ratio in the following form:

$$\begin{aligned} \alpha &\propto (k_s/k_f)^a, \\ C_{dis} &\propto (k_s/k_f)^b, \end{aligned} \tag{30}$$

where a and b are exponents. Our current pore-scale data suggest that $a < 0$ and $b > 0$. For $k_s/k_f = 1$, we will have $\alpha = C_{dis} = k_s/k_f = 1$ when solid and fluid phases have similar thermal conductivities. In other words, the fractional thermal model recovers the classical solution of HRL convection when the contributions from the thermal dispersion due to the thermophysical heterogeneities disappear in HRL convection.

V. DISCUSSION

In the classical advection-diffusion formulation of convection in porous media, the thermal dispersion term $\nabla\cdot((\rho c)_f < \mathbf{V}'T' >^f)$ in Eq. 4 appears as the byproduct of the upscaling and homogenization of the advective transport flux. Despite mathematically having an advective form, closure modeling of the thermal dispersion is

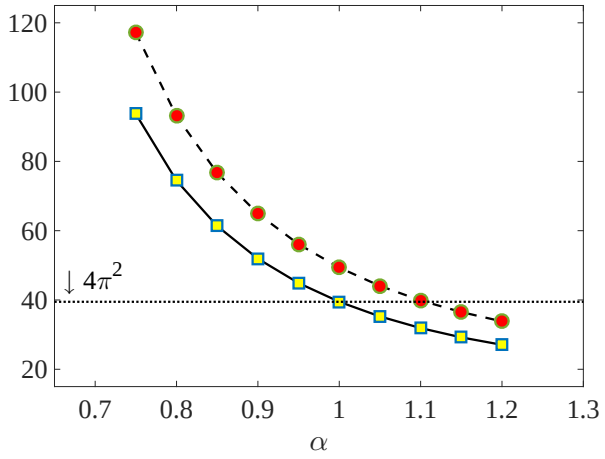

FIG. 3: Comparison of the predicted Ra_{cr} for different values of α based on single-term (lines) and two-term approximation (symbols) in the Galerkin procedure; (—, □) for C_{dis}=1.0, and (−−,○) for C_{dis}=0.8. The horizontal dotted line indicates the classical value of $4\pi^2$ based on integer-order HRL problem.

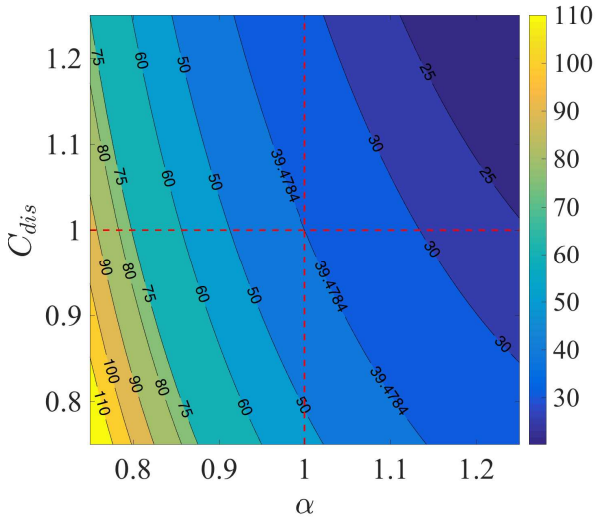

FIG. 4: map showing the variation of Ra_{cr} for different values of α and C_{dis}

commonly based on a nonlinear diffusive term. It can be easily shown that the contribution of a pseudo-diffusive thermal dispersion disappears in the linear stability analysis, therefore it cannot influence the onset of convection [46–48]. Also, the available closure formulations cannot model the consistently lower/higher Nusselt numbers in thermophysically heterogeneous media [47, 49].

The idea behind the fractional-order formulation in Eq. 5 is twofold: (1) we do not assume any *a priori* closure nature to the macroscopic behavior of thermal dispersion, i.e neither pure advective nor pure diffusive but rather a fractional-order term that models the intermediate behaviors in a flexible and consistent manner, and (2)

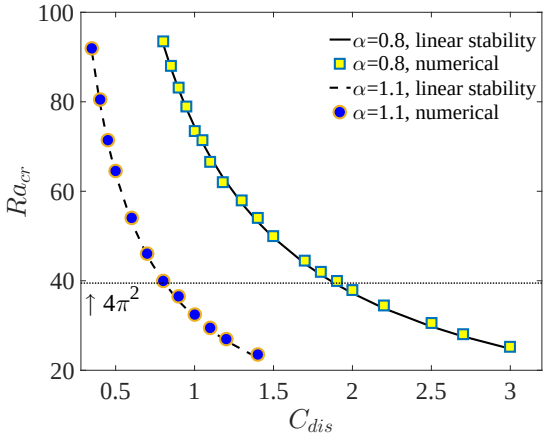

FIG. 5: Comparison of the predicted Ra_{cr} for different dispersivity C_{dis} based on linear stability analysis (lines) and numerical solution of the nonlinear equations (symbols)

we assume that the macroscopic contribution of thermal dispersion in HRL convection, which originates from the upscaling of the advective flux, is to enhance/retard the total advective heat flux due to the thermophysical heterogeneities; a process which cannot be otherwise modeled by the classical advection-diffusion formulation.

The present linear stability and numerical results confirm that including the contribution from the thermal dispersion into a fractional-order advective term not only enables us to model the shift in the onset of convection, but also it successfully provides correct Nusselt-Rayleigh scalings in thermophysically heterogeneous media, in agreement with the pore-scale observations.

While the present linear stability study only accounts for the role of thermophysical heterogeneities on the onset of HRL convection, subsurface systems also include structural and geometrical heterogeneities such as fracture networks. The combined effect of thermophysical and structural heterogeneities will add complexity to the nature of thermal dispersion in HRL convection. It is therefore important to perform theoretical studies and direct numerical simulations for cases where both permeability and thermophysical properties are varying over space, and to investigate how this coupled spatial variation influences the dynamics of HRL convection.

VI. CONCLUSION

This study introduces a fractional-order energy model for studying heat transfer in a density-driven convection in an isotropic and homogeneous porous medium. The fractional-order closure model characterizes the intermediate behaviors between advective and diffusive regimes and accounts for the complex macroscopic realization of transport processes by the thermal dispersion term. We conduct a linear stability analysis to show that the

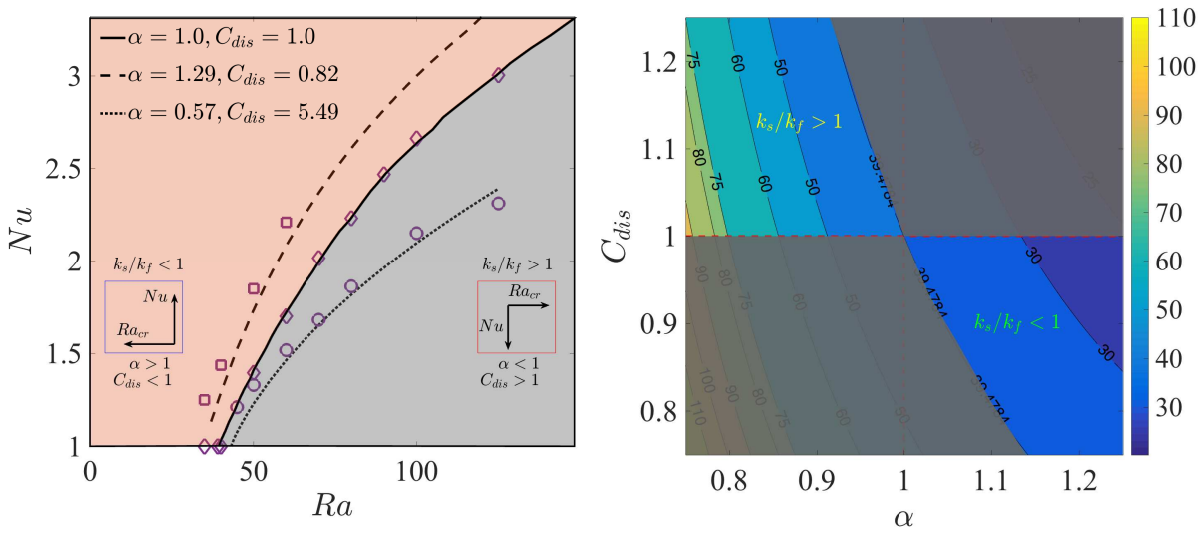

FIG. 6: Panel (a): the dependency of the observed anomalous behaviors in Ra_{cr} and Nusselt-Rayleigh curves on the solid-to-fluid thermal conductivity ratio k_s/k_f. The solid line in Panel (a) is associated with the predictions based on the classical HRL problem with $C_{dis} = \alpha = 1.0$, agreeing with the pore-scale simulations for $k_s/k_f = 1$ ($\diamond$ symbols) [25]. The dashed and dotted curves are the predictions of the fractional-order model qualitatively agreeing with the anomalous behaviors observed in pore-scale results [25] for $k_s/k_f < 1$ ($\square$ symbols) and $k_s/k_f > 1$ ($\circ$ symbols), respectively. Panel (b): valid ranges of C_{dis} and α for satisfying both aspects of anomalous behaviors observed in the pore-scale results [25] for different solid-to-fluid thermal conductivity ratio k_s/k_f. The gray regions in Panel (b) indicate the values of α and C_{dis} out of the suitable ranges for $k_s/k_f < 1$ and $k_s/k_f > 1$ cases.

fractional-order generalization of HRL convection is suitable for modeling the shift on the onset of convection due to the thermophysical heterogeneities in a porous medium; a feature that cannot be captured by the classical formulation of the energy equation. The numerical solution of the complete nonlinear governing flow and temperature equations confirm the validity of the critical Rayleigh numbers found through the linear stability study. To the best of our knowledge, the present thermal fractional-order model is the first of its kind that (1) introduces a new formulation for the macroscopic characterization of thermal dispersion in HRL convection and (2) provides consistent predictions for both the critical Rayleigh number and also Nusselt-Rayleigh scalings in a thermophysically heterogeneous porous medium. The proposed fractional-order thermal model and the linear stability and numerical results suggest new pore-scale simulations over a wide range of thermophysical conditions that can help us to retrieve a meaningful and quantitative relation between fractional-model parameters and thermophysical properties of the medium.

Appendix A: Second approximation Galerkin solution

For the second order approximation, the trial functions take the following form:

$$\begin{aligned}\Psi &= a_{11}\sin(\pi x)\sin(\pi y) + a_{21}\sin(2\pi x)\sin(\pi y) + a_{12}\sin(\pi x)\sin(2\pi y) + a_{22}\sin(2\pi x)\sin(2\pi y),\\ \Theta &= b_{11}\cos(\pi x)\sin(\pi y) + b_{21}\cos(2\pi x)\sin(\pi y) + b_{12}\cos(\pi x)\sin(2\pi y) + b_{22}\cos(2\pi x)\sin(2\pi y).\end{aligned} \tag{A1}$$

We first insert the trial functions A1 in the linearized perturbed equations 20 and 21 to develop the residual equations. We then orthogonalize the residual equations to solve the associated 8×8 generalized eigenvalue problem. The first four equations from the velocity equation are as follows:

$$(m^2+n^2)\pi^2 a_{mn} = m\pi Rab_{mn}, \quad m,n = 1,2. \tag{A2}$$

And the resulting four equations from the energy equation become:

$$-b_{k,l}\frac{(k^2+l^2)\pi^2}{4}+\frac{C_{dis}}{\Gamma(1-\alpha)}\sum_{m=1}^{2}\sum_{n=1}^{2}n\pi a_{mn}\int_0^1\int_0^1(1-y)x^{-\alpha}(\sin(m\pi x)\cos(n\pi y))(\cos(k\pi x)\sin(l\pi y))dxdy$$
$$-C_{dis}\frac{k\pi}{2}\sum_{n=1}^{2}a_{kn}\int_0^1(\frac{y^{-\alpha}}{\Gamma(1-\alpha)}-\frac{y^{-\alpha+1}}{\Gamma(2-\alpha)})\sin(l\pi y)\sin(n\pi y),\quad k,l=1,2. \tag{A3}$$

The set of equations in A2 and A3 results in an 8×8 generalized eigenvalue problem. We use a global search minimization algorithm which identifies the smallest eigenvalue corresponding to the critical Rayleigh number for any specific set of parameters C_{dis} and α.

[1] Y. Zhang, D. A. Benson, and D. M. Reeves, Advances in Water Resources **32**, 561 (2009).
[2] R. Metzler and J. Klafter, Physics Reports **339**, 1 (2000).
[3] J. Klafter and I. M. Sokolov, Physics World **18**, 29 (2005).
[4] R. Klages, G. Radons, and I. M. Sokolov, eds., *Anomalous Transport: Foundations and Applications* (Wiley-VCH Verlag GmbH & Co. KGaA, Weinheim, 2008).
[5] D. A. Benson, S. W. Wheatcraft, and M. M. Meerschaert, Water Resources Research **36**, 1403 (2000).
[6] M. Levy and B. Berkowitz, Journal of Contaminant Hydrology **64**, 203 (2003).
[7] T. Kosztołowicz, K. Dworecki, and S. Mrówczyński, Phys. Rev. Lett. **94**, 170602 (2005).
[8] T. Kosztołowicz, K. Dworecki, and S. Mrówczyński, Phys. Rev. E **71**, 041105 (2005).
[9] R. L. Magin, O. Abdullah, D. Baleanu, and X. J. Zhou, Journal of Magnetic Resonance **190**, 255 (2008).
[10] R. L. Magin, C. Ingo, L. Colon-Perez, W. Triplett, and T. H. Mareci, Microporous and Mesoporous Materials **178**, 39 (2013), proceedings of the 11th Internatioanl Bologna Conference on Magnetic Resonance in Porous Media (MRPM11).
[11] M. Küntz and P. Lavallée, Journal of Physics D: Applied Physics **34**, 2547 (2001).
[12] A. E.-G. E. Abd and J. J. Milczarek, Journal of Physics D: Applied Physics **37**, 2305 (2004).
[13] N. Filipovitch, K. M. Hill, A. Longjas, and V. R. Voller, Water Resources Research **52**, 5167 (2016).
[14] B. I. Henry, T. A. M. Langlands, and S. L. Wearne, Phys. Rev. E **72**, 026101 (2005).
[15] L. Zhang and C. Tian, Phys. Rev. E **90**, 062915 (2014).
[16] R. Torabi and Z. Rezaei, Phys. Rev. E **94**, 052202 (2016).
[17] S. Emmanuel and B. Berkowitz, Transport in Porous Media **67**, 413 (2007).
[18] S. Geiger and S. Emmanuel, Water Resources Research **46** (2010).
[19] Y. Luchko and A. Punzi, GEM - International Journal on Geomathematics **1**, 257 (2011).
[20] A. Suzuki, S. A. Fomin, V. A. Chugunov, Y. Niibori, and T. Hashida, International Journal of Heat and Mass Transfer **103**, 611 (2016).
[21] C. W. Horton and F. T. Rogers, Journal of Applied Physics **16** (1945).
[22] E. R. Lapwood, Mathematical Proceedings of the Cambridge Philosophical Society **44**, 508 (1948).
[23] P. Cheng, Advances in Heat Transfer **14**, 1 (1979).
[24] N. Kladias and V. Prasad, Journal of Thermophysics and Heat Transfer **5**, 560 (1991).
[25] H. Karani and C. Huber, Phys. Rev. E **95**, 033123 (2017).
[26] C. Hsu and P. Cheng, International Journal of Heat and Mass Transfer **33**, 1587 (1990).
[27] J. Levec and R. G. Carbonell, AIChE Journal **31**, 581 (1985).
[28] G. Taylor, Proceedings of the Royal Society of London A: Mathematical, Physical and Engineering Sciences **219**, 186 (1953).
[29] R. Aris, Proceedings of the Royal Society of London A: Mathematical, Physical and Engineering Sciences **235**, 67 (1956).
[30] P. G. Saffman, Journal of Fluid Mechanics **6**, 321349 (1959).
[31] P. G. Saffman, Journal of Fluid Mechanics **7**, 194208 (1960).
[32] M. Poreh, Journal of Geophysical Research **70**, 3909 (1965).
[33] M. M. Meerschaert and A. Sikorskii, *Stochastic Models for Fractional Calculus* (Walter de Gruyter GmbH and Co. KG, 2012).
[34] D. A. Benson, M. M. Meerschaert, and J. Revielle, Advances in Water Resources **51**, 479 (2013).
[35] D. A. Nield and A. Bejan, *Convection in Porous Media* (Springer-Verlag New York, 2013).
[36] I. Podlubny, *Fractional Differential Equations* (Academic Press, 1999).
[37] H. Karani and C. Huber, Journal of Fluid Mechanics **818** (2017), 10.1017/jfm.2017.155.
[38] R. N. Horne, Journal of Fluid Mechanics **92**, 751 (1979).
[39] G. Schubert and J. M. Straus, Journal of Fluid Mechanics **94**, 25 (1979).
[40] P. H. Steen, Journal of Fluid Mechanics **136**, 219 (1983).
[41] D. S. Riley and K. H. Winters, Journal of Fluid Mechanics **204**, 325 (1989).
[42] D. Henry, R. Touihri, R. Bouhlila, and H. Ben Hadid, Water Resources Research **48**, n/a (2012), w10538.
[43] B. A. Finlayson, Journal of Fluid Mechanics **33**, 201208 (1968).
[44] "Convective instability problems," in *The Method of Weighted Residuals and Variational Principles* (1972) Chap. 6, pp. 150–207.
[45] J. L. Beck, Physics of Fluids **15**, 1377 (1972).
[46] H. Neischloss and G. Dagan, The Physics of Fluids **18**, 757 (1975).
[47] O. Kvernvold and P. A. Tyvand, Journal of Fluid Mechanics **99**, 673686 (1980).

[48] C. R. B. Lister, Journal of Fluid Mechanics **214**, 287320 (1990).

[49] J. G. Georgiadis and I. Catton, International Journal of Heat and Mass Transfer **31**, 1081 (1988).